

# Adsorption of Fluorescein on Zr-Pillared Montmorillonite Clays: Studied by Time-Resolved Fluorescence Spectroscopy

**Belbel, Abdeldjabbar\*<sup>+</sup>**

*Department of Chemistry, Ziane Achour University of Djelfa, BP 3117, ALGERIA*

**ABSTRACT:** *In the present study, the adsorption capacities of two intercalated smectites, Na<sup>+</sup>-PMt and Ca<sup>2+</sup>-PMt with the Zr pillar were investigated on fluorescent dye adsorption. The modified clay sample was characterized in detail using X-Ray Diffraction (XRD), and Fourier Transform InfraRed (FT-IR) spectroscopy. The values of interlayer spacing are similar about 16 Å for all samples. The adsorption isotherms fit well with the non-linear Langmuir isotherm model and the maximum adsorption capacities of all materials are determined. For all samples interlayer spacing after interactions between the dye and the modified clay are similar about 18 Å as measured by X-ray diffraction. The pillar improves the adsorption capacity towards fluorescein due to its location inside interlayer space. Interestingly, the time-resolved fluorescence shows that the dye is not released in solution as it is the case for the pristine clay.*

**KEYWORDS:** *Montmorillonite; Zr-pillared clay; Adsorption; Fluorescence.*

## INTRODUCTION

Industries are the main source of water pollution due to release of toxic pollutants that are harmful to humans, animals and water bodies. One of such important pollutant is dyes that are widely used in many industries such as textiles. Some dyes can be carcinogenic and not biodegradable [1]. It is thus needed to find solutions for their removal. Various physicochemical and biological treatment methods have been reported to remove organic dyes from waste water. Adsorption is proven to be a practical way for the treatment of dye waste water due to its efficiency, selectivity and cost-effective nature [2]. The clay minerals have layered structure composed of octahedral and tetrahedral sheets consisting of fine particles of size < 2 µm. Due to their abundance and their

low cost, they have been employed in numerous applications such as adsorbents, catalysts or design membranes [3 - 5].

Among the properties of clay minerals, their ability to swell in water and the presence of both Bronsted and Lewis acidity make them excellent host materials for the full wide diversity of organic molecules [6,7].

To enhance of porosity and active sites and thus the adsorption capacity, surface and structural modifications are required. To do so, various modification processes were reported such as modification with acids [8], polymers [9] alcohols [10], surfactants [11], nanocomposite [12], or doping with metals [13]. Pillared interlayered clays or pillared clays have higher porosity

---

\* To whom correspondence should be addressed.

+ E-mail: belbel.dj@gmail.com

1021-9986/2023/6/1775-1783

9/\$/5.09

than the raw clays due to addition of pillars inside layer the structure, this permanent porosity improving the adsorbent ability. Basically, pillar comes from the rigid cross-linked materials that are obtained by strong binding of metal oxides and aluminosilicate layers using oxygen edges.

Currently, much research interest for inorganic pillared montmorillonites due to more superior porosities [14], thermal stabilities and catalytic activities[15]. The principle of pillaring consists of large inorganic polyhydroxocation species of Al, Zr, Ti, Fe, and Cr (either pure or modified with other cations) intercalated into the clay interlayer, followed by thermal treatment in the temperature range of 300-700 °C [16]. Calcination consisted the important step to prepare pillared clays materials, it results to the dehydroxylation of intercalated pillaring species and their transformation into oxide pillars, thus propping apart the layers of the clays and producing thermally stable rigid cross linked materials with a large surface area, a certain porous texture and acidity [17].

The Zr pillared Mt usually has a large basal spacing and microporous structure, and shows better thermal stability and performance of adsorption for organic compounds and metals than Al pillared one [18], although the chemistry of zirconium in aqueous medium and the factors ruling the species in equilibrium appear somewhat more constraining than for aluminium [19].

The aim of the present work is to investigate the efficiency of different pillared smectite for adsorption of fluorescein (FS). The latter is molecules of Xanthene family are commonly used for broad applications due to the very good quantum efficiency and their photochemical stability. First, the structural properties of pillared clay will be investigated. Then the organic ion location has been studied by XRD. The adsorption isotherms will investigate to evaluate the adsorption mechanism and the adsorption capacities of the pillared clays. For the FS, we also investigate the photophysical properties in aqueous solution by the time resolved fluorescence in order to discuss the releasing processes.

## EXPERIMENTAL SECTION

### Materials

The raw montmorillonite from a Crook County (Wyoming) was purchased from the Source Clays Repository. (Clay mineral Society ref: Srce\_Clay\_SWy-

2), for more details see (<http://www.clays.org/>). This clay mineral has the chemical formula [20]. ( $\text{Si}_{17.89} \text{Al}_{3.34} \text{Fe}_{0.42} \text{Mg}_{0.56} \text{Ca}_{0.52} \text{Na}_{0.14} \text{K}_{0.01}$ ). Its Cation Exchange Capacity (CEC) was reported to be about 75 meq/100 g<sup>-1</sup> [21]. It was used as received without further purification. The majority of the fine particles were mostly smaller than 2 microns in diameter. Homoionic clay of Na<sup>+</sup> and Ca<sup>2+</sup> was obtained as previously reported using 1 M solution of pure (NaCl, 99.8 %), (CaCl<sub>2</sub>, 99.7 %), in deionized water[22]. Sodium fluorescein (FS) (C<sub>20</sub>H<sub>10</sub>O<sub>5</sub>Na<sub>2</sub>, M<sub>w</sub> 376.27 g.mol<sup>-1</sup>; 99.8%, Lot#BCBJ6039V) was purchased from Sigma–Aldrich and used without any further purification.

### Apparatus

Powder XRD analyses were performed on a Panalytical empyrean diffractometer (Netherlands) using Ni-filtered Cu K $\alpha$  as the source of radiation. The samples were all scanned from 3° to 80° with scanning speed of 6° min<sup>-1</sup>. The interlayer distance was calculated, for each sample, from the position of the d<sub>001</sub> ray. FT-IR spectra were analyzed with BIO-RAD FTS-40 Fourier transform infrared in a wave number range of 4000 – 400 cm<sup>-1</sup>. The pressed Potassium bromide (KBr) discs employed for this purpose were prepared using 0.6 mg of sample and 300 mg of KBr.

Time-resolved fluorescence spectroscopy was obtained by the time-correlated single-photon counting technique. The fluorescence decay of FS loaded in different materials was performed in water after removing the FS desorbed in the material. The excitation wavelength was achieved by using a SuperK Extrem high-power white super continuum laser (NTK Photonics, model EXR-15) as a pulsed continuum source. The wave length ( $\lambda=520$  nm) was selected using super KVaria module (NTK Photonics). The repetition rate was set to 38.9 MHz; the excitation pulse duration on this device is around 6 ps (full-width-at-half-maximum, FWHM). For the analysis the fluorescence decay law at the magic angle  $I_M(t)$  was analyzed as a sum of exponentials:

$$I_M(t) = \frac{1}{3} \sum_{i=1}^n \alpha_i e^{(-t/\tau_i)} \quad (1)$$

where  $I(t)$  is the fluorescence intensity,  $\alpha_i$  the pre-exponential factor,  $\tau_i$  the fluorescence lifetime, fluorescence lifetimes were calculated from data collected

at the magic angle by iterative adjustment after convolution of a pump profile (scattered light). with a sum of exponentials as described previously [23].

### Preparation of PMt

The pillaring process consists of two steps. In the first step occur the intercalations of the pillaring agents between host clay layers. In the next stage, these precursors are converted into stable pillars through calcination to reach the final structure of pillared clay is formed in this step-inducing and increase of the interlayer distance.

Zirconium oxychloride ( $ZrOCl_2 \cdot 8H_2O$ , 99.8 %, S.D. Fine-Chem Ltd.) in aqueous solution (0.1 M, pH 1.43) was first aged at 40 °C for 1 h. In a typical procedure to intercalated Zr, 3 g of the homoionic Mt (Mt-Na or Mt-Ca) was dispersed in 300 mL of deionized water. The amount of pillared clays with Zr solution required to obtain a Zr/Mt ratio of 10 mmol/g was then added drop wise to the clay slurry [24]. Then, the mixture was kept under constant stirring for 1 h. The suspension was centrifuged and washed with distilled water until reaching free of chloride ions. The pillared clay was noted  $Na^+$ -PMt and  $Ca^{2+}$ -PMt according to the exchangeable cation.

### Dye adsorption on Material

Sodium fluorescein. It was adsorbed on the materials as follows: 10 mg (or 30 mg for the kinetic study) of zirconium pillared montmorillonite  $Na^+$ -PMt-or  $Ca^{2+}$ -PMt was dispersed in 10 mL (or 30 mL for the kinetic study) of fluorescein sodium solution (FS) with concentrations from 60 to 300  $\mu\text{mol} \cdot \text{L}^{-1}$  for the isotherm study (or 50  $\mu\text{mol} \cdot \text{L}^{-1}$  for the kinetic study). The mixture was stirred for 20 min at 240 rpm at room temperature. For kinetic study, the contact time was from 5 to 60 min by 5 min step. After that, the mixture was centrifuged in 2000 rpm for 5 min to separate the adsorbent. The fluorescein concentration in the supernatant was measured by absorbance at 489 nm using UV-visible spectrophotometer (UviLine 9400-SECOMAM). The calibration was performed using standard solutions of fluorescein concentration range 7.5 to 30  $\mu\text{M}$  with a regression coefficient of 0.997.

## RESULTS AND DISCUSSION

### X-ray Diffraction Analyses

The starting host clay  $Na^+$ -Mt,  $Ca^{2+}$ -Mt exhibited an interlayer spacing of 12.22 Å and 14.96 Å respectively,

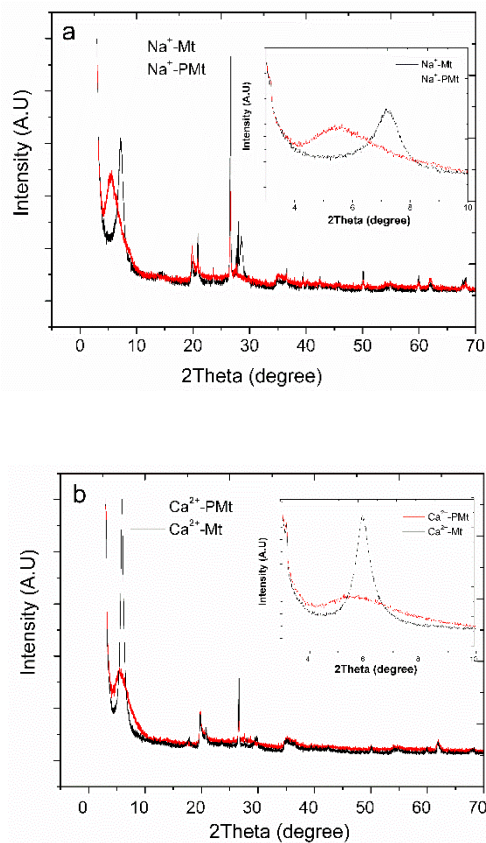


Fig. 1: XRD patterns of Mt samples :before and after ntercalated with Zr-pillaring , a)  $Na^+$ -Mt, and b)  $Ca^{2+}$ -Mt.

confirming that the Ca and Na, were major cations that were exchangeable in the starting clay [25]. After reaction with Zirconium oxychloride Fig.1), interlayer spacing of the samples  $Na^+$ -PMt and  $Ca^{2+}$ -PMt increased to 16.05 Å and 16.56 Å respectively due to the presence of zirconium pillaring species [26,27] .

These values are in good agreement with the one reported in the literature for Zr-pillared clays [23]. When the pillared clays adsorbed anionic dye, an expansion of 18 Å was achieved (Fig.2).

This confirms that the fluorescein is intercalated inside interlayer space. Table1 gives the basal spacing values characterising for all samples.

### FT-IR analysis

The infrared spectra of pillared clay are shown in Fig.3. The most distinctive feature of the Mt spectrum is the broad absorption band that ranges from 3400 to 3600  $\text{cm}^{-1}$ . The band at 3617  $\text{cm}^{-1}$  is characteristic of OH vibration

Table 1: Basal spacing of all samples.

basal spacing (Å)	Ca <sup>2+</sup> -Mt	Na <sup>+</sup> -Mt
Homoionic- Mt	14.96	12.22
PMt	16.56	16.05
PMt-FS	17.90	18.43

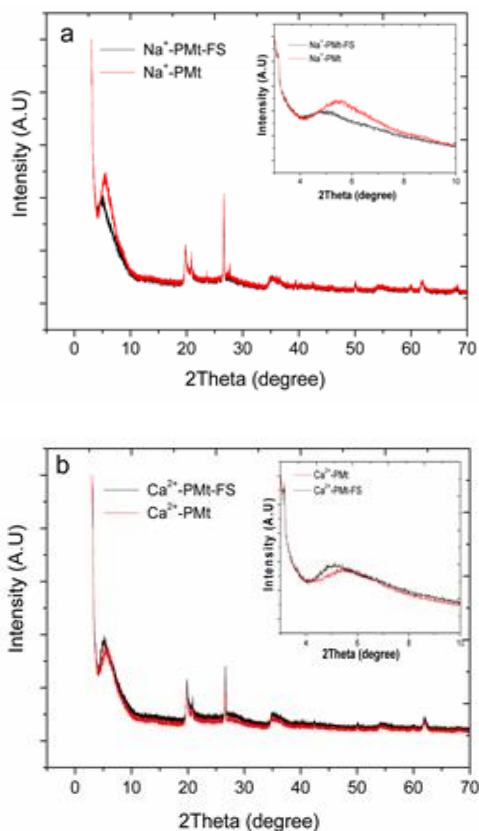


Fig. 2: X-ray diffraction patterns of PMt samples before and after adsorption of fluorescein, a) Na<sup>+</sup>-PMt and b) Ca<sup>2+</sup>- PMt.

of smectite. The band at 3426 cm<sup>-1</sup> was due to OH stretching of water molecules adsorbed in the interlayer region of the clay. The adsorption band at 1637 cm<sup>-1</sup> is attributed to the deformational vibrations of adsorbed water molecules [28].

The large band observed at 1044 cm<sup>-1</sup> all the spectra, were attributed to the Si-O stretching vibration of montmorillonite [29]. The angular deformation bands at 522 and 459 cm<sup>-1</sup> are attributed to the Si-O-M type bonds (M =Mg, Al or Fe) [30,31]. The intensity of the peak observed at about 3426 cm<sup>-1</sup> was higher than that of the homoionic clays due to the presence of hydroxy-Zr species

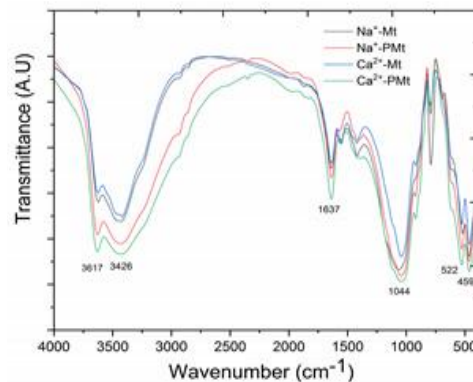


Fig. 3: Infrared spectra of Mt samples: before and after intercalated with Zr-pillaring.

and hydroxyl groups involved in water-water hydrogen bonds [32]. However, in our case, the peak corresponding to the bending vibration of water molecules at 1637 cm<sup>-1</sup> was also increased in intensity. The similarity of the FT-IR spectra between the Mt and PMt designated that the basic structure of the clay was not altered during the pillaring process.

#### Adsorption Kinetics

The kinetic study aims to investigate the time needed to reach equilibrium for adsorption of FS onto modified clays so that future studies could be unified into a fixed time by which equilibrium would be established. For Ca<sup>2+</sup>-PMt and Na<sup>+</sup>-PMt, the time to reach equilibrium was 20 minutes. The experiment data were fitted to several kinetic models and the pseudo-second order kinetic is confirmed by fitting  $t/q_t$  (where  $q_t$  is amount of FS removed,  $t$  denotes time) into a straight line. The pseudo second-order kinetic model is given by the following equation:

$$\frac{dq_t}{dt} = k(q_e - q_t)^2 \quad (2)$$

Where  $K$  (g/mg.min) represent the rate constant of the pseudo-second-order Kinetic model,  $q_e$  (mg/g)

and  $q_e$  (mg/g) are the amounts of solute adsorbed per gram of adsorbent at any time and at equilibrium, respectively. Integration for boundary conditions  $t = 0$  to  $t = t$  and  $q_t = 0$  to  $q_t = q_t$  follow by rearrangement gives:

$$q_t = \frac{Kq_e^2 \cdot t}{1 + Kq_e \cdot t} \tag{3}$$

The equation (2) can be rearranged linear forms as:

$$\frac{t}{q_t} = \frac{1}{kq_e^2} + \frac{1}{q_e} t \tag{4}$$

The results obtained in (Fig.4), show that the adsorption kinetics conforms to a pseudo-second-order equation. From Table 2, the calculated values of coefficient  $R^2$  is up to 0.99. From these results, we can deduce that the studied adsorption system well meets the pseudo-second-order kinetic model.

**Isotherm Studies**

Adsorption isotherm models play an important role in the determination of the maximum capacity of adsorption, and clearly depict the relationship of the amount of dyes adsorbed by a unit weight of the clays at equilibrium. The equilibrium adsorption isotherm explains how the dye interacts with the clay, and how the adsorbate distributes between the solution ( $C_e$ ) and the solid phase ( $q_e$ ) when the adsorption process reaches the equilibrium state. Adsorption isotherm models such as Langmuir [33], and Freundlich [34] .were commonly used to describe the experimental data [35]. The Langmuir adsorption isotherm is based on the assumption that the monolayer adsorption onto a surface containing a finite number of adsorption sites. It also assumes uniform energies of adsorption as well as no mutual interaction between the adsorbed molecules. The non-linear equation of the Langmuir isotherm model is expressed by Eq (5):

$$q_e = \frac{K_L q_m C_e}{1 + K_L C_e} \tag{5}$$

where  $q_m$  is the maximum monolayer adsorption capacity,  $K_L$  the Langmuir equilibrium constant. The essential characteristics of the Langmuir isotherm parameters can be expressed in terms of a dimensionless constant called the separation factor, or a dimensionless equilibrium parameter,  $R_L$  [36]. The dimensionless constant  $R_L$  is the essential characteristic of the Langmuir isotherm and it can be expressed by Eq. (6):

**Table 2: Parameters obtained from the analysis of adsorption kinetics by the Pseudo-second-order model.**

Pseudo-second-order model			
Sample	$q_{eq}$ (mg/g)	$K$ (g/mg.min)	$R^2$
Ca <sup>2+</sup> -PMt	15.673	0.905	0.999
Na <sup>+</sup> -PMt	10.438	1.996	0.991

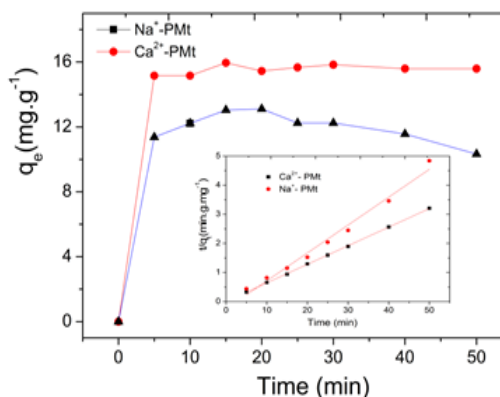


**Fig. 4: The effect of contact time on dye adsorption by modified montmorillonite. Inserts are plot of  $t/q_t$  against  $t$ .**

$$R_L = \frac{1}{1 + K_L C_0} \tag{6}$$

The Freundlich isotherm is based on the assumption that adsorption occurs on a heterogeneous adsorption surface with different energies of adsorption and is given by the Eq (7):

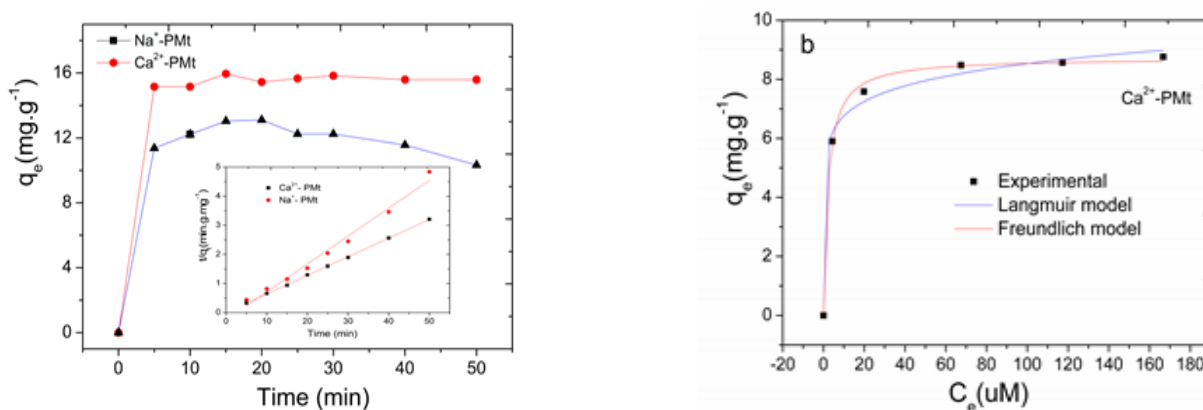
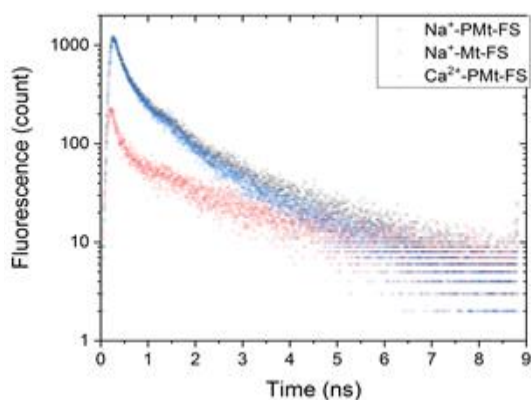
$$q_e = K_f C_e^{\frac{1}{n}} \tag{7}$$

Where  $K_f$  and  $n$  are the Freundlich constants related to the adsorption capacity and adsorption intensity respectively. The value of  $1/n$  that varies between 0.1 to 1.0 indicates the favourable adsorption of molecule.  $n$  is a measure of the deviation of the adsorption isotherm linearity.

According to the  $R^2$ , the Langmuir model is the most suitable to describe the experimental data. The calculated  $R_L$  values based on the Langmuir adsorption isotherm are close to 0.1 indicating that the adsorption process is strongly favourable. In addition, the maximum adsorption capacities and the best affinity are obtained for Na<sup>+</sup>-PMt. Indeed the FS adsorbed on PMt were 21.53 mg/g ,8.72 mg/g for Na<sup>+</sup>-PMt and Ca<sup>2+</sup>-PMt respectively (Table 3, Fig.5).

Table 3: Fitting parameters obtained for Langmuir and Freundlich isotherms.

Langmuir model				Freundlich model			
Adsorbent	$q_m(\text{mg}\cdot\text{g}^{-1})$	$K_L(\text{L}/\text{mg}^1)$	$R^2$	$R_L$	$K_F(\text{mg}\cdot\text{g}^{-1})$	n	$R^2$
$\text{Ca}^{2+}$ -PMt	8.721	0.461	0.998	0.087-0.022	5.395	10	0.987
$\text{Na}^+$ -PMt	21.53	0.075	0.994	0.371-0.124	4.544	3.225	0.973

Fig.5: Adsorption isotherm of fluorescein on PMt and fit using Langmuir and Freundlich model, a)  $\text{Na}^+$ -PMt and b)  $\text{Ca}^{2+}$ -PMt.Fig.6: Fluorescence decay of fluorescein loaded on:  $\text{Na}^+$ -Mt (red),  $\text{Ca}^{2+}$ -PMt (blue) and  $\text{Na}^+$ -PMt (black).

These values of adsorption capacity are higher than the one previously reported for FS in same montmorillonite ( $2.713 \text{ mg}\cdot\text{g}^{-1}$ ) [37]. On the other hand, for the anionic dye such as rhodamine or sulforhodamin the clay is not satisfactory because the dye is more easily released [38,39]. At this stage, the pillared clays seem to be a good candidate for removal of fluorescein.

### Impact of Clays on Photophysical Properties of Fluorescein Dye

In order to characterize the clay-fluorescein interactions, the photophysical properties of dye were studied by time resolved fluorescence in aqueous solution. The fluorescence decay was reported in (Fig.6) and the results are summarized in Table 4.

Free in solution, the fluorescence decay of fluorescein can be fitted with a single exponential function with a lifetime  $\tau=3.82 \text{ ns}$ . When the fluorescein loaded on Na-Mt where 65 % of the fluorescence come from a lifetime about 3.70 ns (closer than the one free in solution).

This suggests that the dye is surrounded by water molecules and thus not adsorbed on the clay surface. Such releasing of the dye was also previously reported for the Mt-BMIM [37].

For the fluorescein loaded on the pillared clay, a decrease of the average life time to 1.19 ns and 1.02 ns were observed for  $\text{Ca}^{2+}$ -PMt  $\text{Na}^+$ - PMt respectively. The modification of the fluorescence emission can be assigned to the strong interaction between the pillared clay and the dye [40]. This could confirm the location of the dye inside the interlayer space of the clay.



**Table 4: Fluorescent lifetime ( $\tau_i$ ) and yield for dye adsorbed in Mt Al (Yield =  $100 \text{ airci}/\Sigma \text{airci}$  represents the contribution of each emission to the total emission).**

	$\tau_1$ (ns) (Yield)	$\tau_2$ (ns) (Yield)	$\tau_3$ (ns) (Yield)	$\tau_{Av}$ (ns)	$\chi^2$
Free	3.82 (100%)			3.82	1.05
Mt-Na	3.70 (65.7%)	0.733 (21.1%)	0.08 (12%)	2.60	1.1
Na <sup>+</sup> -PMt-FS	2.39 (37.0%)	0.66 (41.9%)	0.128 (21.1%)	1.19	1.07
Ca <sup>2+</sup> - PMt-FS	2.1 (35.2%)	0.58 (43.9%)	0.10 (20.9%)	1.02	1.14

## CONCLUSIONS

Two different pillared interlayered clays Na<sup>+</sup>-PMt and Ca<sup>2+</sup>-PMt were prepared using a conventional method consisting in two steps. The adsorption isotherm results showed that the affinity of dye is limited for adsorption capacities range from 9 mg g<sup>-1</sup> to 22 mg g<sup>-1</sup>. The XRD patterns indicate an intercalation of the Zr agent in the interlayer space. In addition, the pillar enhances the adsorption capacity fluorescein due to its location inside interlayer space. Interestingly, the time resolved fluorescence show that the dye is not released in solution as it is the case for the pristine clay. Our work demonstrates that the pillared clay could be a good candidate to remove anionic dyes from water without the releasing effect previously demonstrated for clay minerals. In addition, the modification of the fluorescence lifetime due to the interaction with the material could also find applications as new pigment. Regardless the application, we believe that the intercalation of anionic dye inside pillared clay is interesting and exciting field to investigate.

Received : May 7, 2022 ; Accepted : Oct. 10, 2022

## REFERENCES

- [1] Vidhyadevi T., Murugesan A., Kirupha S.D., Baskaralingam P., Ravikumar L., Sivanesan S., Adsorption of Congo Red Dye over Pendent Chlorobenzylidene Rings Present on Polythioamide Resin: Kinetic and Equilibrium Studies, *Sep. Sci. Technol. (Philadelphia)*, **48(10)**: 1450–1458 (2013).
- [2] Vidhyadevi T., Murugesan A., Kalaivani S.S., Anil Kumar M., Thiruvankada Ravi K.V., Ravikumar L., Anuradha C.D., Sivanesan S., Optimization of the Process Parameters for the Removal of Reactive Yellow Dye by the Low Cost *Setaria Verticillata* Carbon Using Response Surface Methodology: Thermodynamic, Kinetic, and Equilibrium Studies, *Environ. Prog. Sustain. Energy*, **33(3)**: 855–865 (2014).
- [3] Jaber M., Georgelin T., Bazzi H., Costa-Torro F., Lambert J.-F., Bolbach G., Clodic G., Selectivities in Adsorption and Peptidic Condensation in the (Arginine and Glutamic Acid)/Montmorillonite Clay System, *J. Phys. Chem., C*, **118(44)**: 25447–25455 (2014).
- [4] Fournier F., Viguerie L. de, Balme S., Janot J.-M., Walter P., Jaber M., Physico-Chemical Characterization of Lake Pigments Based on Montmorillonite and Carminic Acid, *J. Appl. Clay Sci.*, **130**: 12–17 (2016).
- [5] Kamgang-Syapnjeu P., Njoya D., Kamseu E., Cornette de Saint Cyr L., Marcano-Zerpa A., Balme S., Bechelany M., Soussan L., Elaboration of a New Ceramic Membrane Support from Cameroonian Clays, Coconut Husks and Eggshells: Application for *Escherichia Coli* Bacteria Retention, *J. Appl. Clay Sci.*, **198**: 105836 (2020).
- [6] Lepoitevin M., Jaber M., Guégan R., Janot J.-M., Dejardin P., Henn F., Balme S., BSA and Lysozyme Adsorption on Homoionic Montmorillonite: Influence of the Interlayer Cation, *J. Appl. Clay Sci.*, **95**: 396–402 (2014).
- [7] Adraa K. El, Georgelin T., Lambert J.-F., Jaber F., Tielens F., and Jaber M., Cysteine-montmorillonite composites for heavy metal cation complexation: A combined experimental and theoretical study, *Chem. Eng. J.*, **314**: 406–417 (2017).
- [8] Vengris T., Binkien R., Sveikauskait A., Nickel, copper and zinc removal from waste water by a modified clay sorbent, *J. Appl. Clay Sci.*, **18 (3-4)**: 183–190 (2001).
- [9] Liu P., Polymer Modified Clay Minerals: A review, *Appl. Clay Sci e.*, **38 (1-2)**: 64–76 (2007).
- [10] Seydibeyoglu M. O., Demiroglu S., Atagur M., and Ocaktan S. Y., Modification of Clay Crystal Structure with Different Alcohols, *Nat. Resour. Res.*, **08 (11)**: 709–715 (2017).

- [11] Krishna B.S., Murty D.S.R., Jai Prakash B.S., [Surfactant-Modified Clay as Adsorbent for Chromate](#), *J. Appl. Clay Sci.*, **20(1-2)**: 65–71 (2001).
- [12] Sharma S. K. and Nayak S. K., [Surface Modified Clay/Polypropylene \(PP\) Nanocomposites: Effect on Physico-Mechanical, Thermal and Morphological Properties](#), *Polym. Degrad. Stab.*, **94(1)**: 132–138 (2009).
- [13] Nguyen-Thanh D., Block K., Bandosz T.J., [Adsorption of Hydrogen Sulfide on Montmorillonites Modified with Iron](#), *Chemosphere.*, **59(3)**: 343–353 (2005).
- [14] Cooper C., Jiang J.-Q., Ouki S., [Preliminary Evaluation of Polymeric Fe- and Al-Modified Clays as Adsorbents for Heavy Metal Removal in Water Treatment](#), *J. Chem. Technol. Biotechnol.*, **77(5)**: 546–551 (2002).
- [15] Molina C.B., Casas J.A., Zazo J.A., Rodríguez J.J., [A Comparison of Al-Fe and Zr-Fe Pillared Clays for Catalytic Wet Peroxide Oxidation](#), *Chem. Eng.*, **118(1-2)**: 29–35 (2006).
- [16] "Pillared Clays and Related Catalysts", Springer. New York: New York, NY (2010).
- [17] Klopogge J.T., Duong L.V., Frost R.L., [A Review of the Synthesis and Characterisation of Pillared Clays and Related Porous Materials for Cracking of Vegetable Oils to Produce Biofuels](#), *Environ.*, **47(7)**: 967–981 (2005).
- [18] Zhu M.-X., Ding K.-Y., Xu S.-H., Jiang X., [Adsorption of Phosphate on Hydroxyaluminum- and Hydroxyiron-Montmorillonite Complexes](#), *J. Hazard. Mater.*, **165(1-3)**: 645–651 (2009).
- [19] Moreno S., Kou R.S., Molina R., Poncelet G., [Al-, Al,Zr-, and Zr-Pillared Montmorillonites and Saponites: Preparation, Characterization, and Catalytic Activity in Heptane Hydroconversion](#), *J. Catal.*, **182(1)**: 174–185(1999).
- [20] Mermut A.R., Lagaly G., [Baseline Studies of the Clay Minerals Society Source Clays: Layer-Charge Determination and Characteristics of Those Minerals Containing 2:1 Layers](#), *J. Clays Clay Min.*, **49(5)**: 393–397(2001).
- [21] Olphen H. Van, Fripiat J.J., [Organisation for Economic Co-operation and Development. , and Clay Minerals Society, Data Handbook for Clay Materials and other Non-Metallic Minerals](#) , 346 (1979).
- [22] Haouzi A., Kharroubi M., Belarbi H., Devautour-Vinot S., Henn F., Giuntini J.C., [Activation Energy For Dc Conductivity in Dehydrated Alkali Metal-Exchanged Montmorillonites: Experimental Results and Model](#), *J. Appl. Clay Sci.*, **27(1-2)**: 67–74 (2004).
- [23] Balme S., Janot J.-M., Déjardin P., Seta P., [Highly Efficient Fluorescent Label Unquenched by Protein Interaction to Probe the Avidin Rotational Motion](#), *J. Photochem. Photobiol. A.*, **184(1-2)**: 204–211 (2006).
- [24] Bahranowski K., Włodarczyk W., Wisła-Walsh E., Gaweł A., Matusik J., Klimek A., Gil B., Michalik-Zym A., Dula R., Socha R.P., Serwicka E.M., [\[Ti,Zr\]-pillared montmorillonite – A New Quality with Respect to Ti- and Zr-Pillared Clays](#), *J. Microporous Mesoporous Mater.*, **202**: 155–164 (2015).
- [25] Kharroubi M., Balme S., Haouzi A., Belarbi H., Sekou D., Henn F., [Interlayer Cation–Water Thermodynamics and Dynamics in Homoionic Alkali and Alkaline-Earth Exchanged Montmorillonites with Low Water Loadings](#), *J. Phys. Chem. C.*, **116(28)**: 14970–14978 (2012).
- [26] Ohtsuka K., Hayashi Y., Suda M., [Microporous Zirconia-Pillared Clays Derived from Three Kinds of Zirconium Polynuclear Ionic Species](#), *Chem. Mater.*, **5(12)**: 1823–1829 (1993).
- [27] Singh V., Sapehiyia V., Kad G.L., [Ultrasound and Microwave Activated Preparation of ZrO<sub>2</sub>-pillared Clay Composite: Catalytic Activity for Selective, Solventless Acylation of 1,n-Diols](#), *J. Mol. Catal. A Chem.*, **210(1-2)**: 119–124 (2004).
- [28] Kooli F., Yan, L., Tan S.X., Zheng J., [Organoclays from Alkaline-Treated Acid-Activated Clays](#), *J. Therm. Anal. Calorim.*, **115(2)**: 1465–1475 (2014).
- [29] Lerot L., [Effect of Swelling on the Infrared Absorption Spectrum of Montmorillonite](#), *J. Clays Clay Min.*, **24(4)**: 191–199 (1976).
- [30] Huang Z.-M., Zhang Y.-Z., Kotaki M., Ramakrishna S., [A Review on Polymer Nanofibers by Electrospinning and their Applications in Nanocomposites](#), *Compos. Sci. Technol.*, **63(15)**: 2223–2253 (2003).
- [31] Greiner A., Wendorff J.H., [Electrospinning: A Fascinating Method for the Preparation of Ultrathin Fibers](#), *Angew. Chem*, **46(30)**: 5670–5703 (2007).



- [32] Bodoardo S., Chiappetta R., Onida B., Figueras F., Garrone E., [Ammonia Interaction and Reaction with Al-Pillared Montmorillonite: An IR Study](#), *J. Microporous Mesoporous Mater.*, **20(1-3)**: 187–196 (1998).
- [33] Langmuir I., [The Adsorption of Gases on Plane Surfaces of Glass, Mica And Platinum](#), *J. Am. Chem. Soc.*, **40(9)**: 1361–1403 (1918).
- [34] Freundlich H.M.F., [“Over the Adsorption in Solution,”](#) *The Journal of Physical Chemistry*, **57**: 385–471(1906).
- [35] Benetoli L.O. de B. , Santana H. de , Zaia C.T.B.V , Zaia D.A.M., [Adsorption of Nucleic Acid Bases on Clays: An Investigation using Langmuir and Freundlich Isotherms and FT-IR Spectroscopy](#), *Monatsh. Chem.*,**139(7)**: 753–761 (2008).
- [36] Vidhyadevi T., Arukkani M., Selvaraj K., Periyaraman P.M., Lingam R., Subramanian S., [A Study on the Removal of Heavy Metals and Anionic Dyes from Aqueous Solution by Amorphous Polyamide Resin Containing Chlorobenzalimine and Thioamide as Chelating Groups](#), *Korean J. Chem. Eng.*,**32(4)**: 650–660 (2015).
- [37] Belbel A., Kharroubi M., Janot J.-M., Abdessamad M., Haouzi A., Lefkaier I.K., Balme S., [Preparation and Characterization of Homoionic Montmorillonite Modified with Ionic Liquid: Application in Dye Adsorption](#), *Colloids Surf. A Physicochem. Eng. Asp.*, **558**: 219–227 (2018).
- [38] Tangaraj V., Janot J.-M., Jaber M., Bechelany M., Balme S., [Adsorption and Photophysical Properties of Fluorescent Dyes over Montmorillonite and Saponite Modified by Surfactant](#), *Chemosphere.*, **184**: 1355–1361(2017).
- [39] Tangaraj V., Murugesan A., Kalaivani S., Premkumar M.P., Ravikumar L.,Sivanesan S., [A Study on the Removal of Heavy Metals and Anionic Dyes from Aqueous Solution bBy Amorphous Polyamide Resin Containing Chlorobenzalimine and Thioamide Aschelating Groups.](#), *Korean J. Chem. Eng.*, **32**: 650–660 (2015).
- [40] Trigueiro P., Pereira F.A.R., Guillermin D., Rigaud B., Balme S., Janot J.-M., Santos I.M.G. dos., Fonseca M.G., Walter P., Jaber M., [When Anthraquinone Dyes Meet Pillared Montmorillonite: Stability or Fading Upon Exposure to Light?](#), *Dyes Pigm.*, **159**: 384–394 (2018).